Substrate effects on the thermal conductivity of epitaxial graphene nanoribbons

Zhi-Xin Guo,[1,*] J. W. Ding,[1,2] and Xin-Gao Gong[3]
[1]*Department of Physics, Xiangtan University, Xiangtan, Hunan 411105, China*
[2]*College of Electronic Science Engineering, Nanjing University of Post & Telecommunication, 211106, Nanjing, China*
[3]*Key Laboratory for Computational Physical Sciences (MOE) and Surface Physics Laboratory, Fudan University, Shanghai 200433, China*
(Received 13 February 2012; published 13 June 2012)

We study the effect of SiC substrate on thermal conductivity of epitaxial graphene nanoribbons (GNRs) using the nonequilibrium molecular dynamics method. We show that the substrate has strong interaction with single-layer GNRs during the thermal transport, which largely reduces the thermal conductivity. The high thermal conductivity of suspended GNRs is obtained in the second layers of bilayer GNRs, which has a weak van der Waals interaction with the underlying structures. The out-of-plane phonon mode is found to play a critical role on the thermal conductivity variation of the second GNR layer induced by the underlying structures. The effect of disordered edge defects on thermal conductivity is further investigated. The results show that the disordered edge defects can remarkably decrease thermal conductivity of GNRs weakly interacted with substrate, while the effect becomes minor on GNRs strongly interacted with substrate.

DOI: 10.1103/PhysRevB.85.235429 PACS number(s): 65.80.Ck, 61.48.Gh, 44.10.+i, 63.22.Rc

I. INTRODUCTION

Graphene and graphene nanoribbons (GNRs) are thought to be ideal materials for nanoelectronics due to their outstanding electronic and thermal properties.[1–6] In the production the graphene nanomaterials can be either prepared by mechanical exfoliation from graphite[7,8] or by epitaxial growth on SiC substrate.[9,10] The mechanical method is quite delicate and time consuming, which makes it unapplicable in the industry. The epitaxial growth method is nowadays commonly accepted to represent a viable method of controllable growth for the fabrication of high quality graphene wafers.[11] The electronic properties of epitaxial graphene on SiC substrate had been extensively studied.[10,12–14] It was found the electronic properties of graphene can be well preserved in both the single-layer (SL) graphene on SiC $(000\bar{1})$ (C-terminated),[10] and the second layer of bilayer (BL) graphene on SiC (0001) (Si-terminated),[12,13] having great application potential in nanoelectronics. Since the heat removal is a crucial issue in the nanoelectronic industry, the thermal conduction property of epitaxial graphene and GNRs becomes particularly important to its application in nanoelectronics.

During the last two years the thermal conductivity of exfoliated graphene on different substrates (SiO2, Cu) has been extensively studied, where only weakly coupled graphene-substrate interaction exists.[15–19] Different from the exfoliated graphene case, the epitaxial graphene-substrate interaction is much more complicated, and both covalently bonded and weakly coupled GNR-substrate interactions were experimentally observed.[10,20] Thus the thermal conductivity of epitaxial graphene and GNRs is expected to be very different from the exfoliated ones.

In this work we use the nonequilibrium molecular dynamics (NEMD)[6,21–23] method to study the thermal conductivity of epitaxial GNRs on 4H-SiC $(000\bar{1})$ and (0001) surface. On the $(000\bar{1})$ surface, both covalently bonded and weakly coupled GNR-substrate interaction conditions are considered. On the (0001) surface we consider both the SL and BL GNR-substrate interaction cases. In the BL GNR we concentrate on the thermal conductivity of the second layer since the first layer is expected to have similar thermal conductivity as the SL GNR. Two typical GNRs, that is, armchair GNR (AGNR) and zigzag GNR (ZGNR), are considered, and we refer to AGNR/ZGNR with N dimer lines in width as N-AGNR/N-ZGNR for convenient representation.[24]

II. METHODOLOGY

A. Background

The theoretical treatment of the thermal conductivity of graphene/GNR can be roughly divided into two groups. The first is the molecular dynamics (MD) simulations, which utilize the Tersoff/Brenner empirical potentials for C-C interactions and NEMD/EMD simulations for the extraction of the thermal conductivity.[5,6,19] MD can give good results at high temperatures, while it is not correct at low temperatures due to its failure in describing the Bose-Einstein phonon distributions and ballistic phonon transport.[25,26] The thermal conductivity predicted by MD is also affected by the adopted empirical potentials and the simulated system size,[6,22,27] The second is based on the solution of the Boltzmann equations with the phonon scattering rates determined from the perturbation theory or fitted to the experimental data, which is commonly referred to as Callaway-Klemens.[28–32] The *ab initio* method (a quantum mechanical based method) can be applied to calculate the phonon spectra in the second method, which is expected to give more accurate results than the empirical potential method.[30,31] While the accuracy of the second method can also vary depending on the assumptions, particularly in the treatment of Umklapp processes. Because of the computational expense, the studied graphene/GNR by MD method is usually within 100-nm scale.[5,6,19,33,34] Thus the reported thermal conductivity by MD method is usually lower than that reported by Boltzmann equation based methods, which usually consider the graphene/GNR size to be micrometer scale.

Since the graphene/GNR with substrate is a complex system containing many atoms in a unit cell,[35] it is hard to calculate the phonon spectra directly from the quantum mechanical based

methods, and no such study has been reported so far. MD is an ideal choice to treat the large-complex nanosystems. In this paper we use the MD to investigate thermal conductivity of GNRs on SiC at room temperature (300 K), where the quantum effect is expected to be minor.

The parameters of empirical interatomic potentials are usually obtained by fitting the cohesive energy and lattice constant of experimental and *ab initio* results. There may be some divergence on the force constant and the phonon spectra results between the empirical potential and *ab initio* methods. We have calculated the force constants of Si-C and C-C dimmers in use of both Tersoff[36] potential and the *ab initio* (RSDFT)[37] calculations. The force constant of Si-C(C-C) dimmer obtained by Tersoff potential is 3.7(6.4) N/cm, larger than obtained by the *ab initio* calculation, which has a value of 2.0(4.9) N/cm. This indicates the Tersoff potential overestimates the stiffness of C-C and C-Si bonds and thus the phonon frequencies compared with the *ab initio* results. We also have calculated the phonon spectra of graphene using the Tersoff potential. Compared with the *ab initio* results,[38] it is found the overestimation of phonon spectra mainly appears in the optical phonon modes, the frequencies of which are higher than 900 cm^{-1}. Since the thermal conductivity at room temperature is mainly attributed to the low-frequency phonons, we expect the Tersoff potential to overestimate thermal conductivity to a small extent, and it does not affect the general picture of heat transport.

B. MD simulation details

The 4H-SiC substrate is modeled with four alternating Si and C atomic layers. One Si-C layer at the bottom of the sample is fixed. GNRs are placed on top of the SiC substrate, with infinite length along the X direction and finite width along Y direction. The smallest cell of the GNR-SiC system is of 10.12 nm in length (X direction) and 2.15 nm (around 1 nm) for the SiC (GNR) in width (Y direction), containing 2128 SiC atoms and 320 (368) 4-ZGNR (8-AGNR) atoms, respectively.

In the geometry optimization, periodic boundary conditions are applied both along the X and Y directions. We use the Tersoff potential to describe the C-C and C-Si bonded interactions, and the nonbonded van der Waals interaction is described by the Lennard-Jones (LJ) potential[39] in the region where the distance between GNR and SiC atoms is larger than 3.2 Å. In the intermediate, the atomic interaction is described by a cubic spline function.[40]

In the NEMD simulation we employ the velocity Verlet method to integrate equations of motion with a fixed time step of 1 fs. Fixed boundary condition is applied along the X direction, where the outmost layers of each end of GNR (SiC) are fixed. Next to the boundaries, the adjacent 1-nm-long GNR (SiC) layers are coupled to the Nosé-Hoover[41] thermostats with temperatures 310 and 290 K, respectively. The thermal conductivity of GNRs κ is then calculated from the Fourier law,

$$\kappa = -\frac{J_1}{\nabla T \cdot V}. \tag{1}$$

J_1 is the total heat flux along length (X) direction except for the two ends that coupled to the thermostats, which can be obtained from the Green-Kubo relation[27,42]:

$$J_1(t) = \sum_i v_{i,1}\varepsilon_i + \frac{1}{2}\sum_{ij,i\neq j} r_{ij,1}(\mathbf{F}_{ij}\cdot\mathbf{v}_i) + \frac{1}{6}\sum_{ijk}(r_{ij,1}+r_{ik,1})(\mathbf{F}_{ijk}\cdot\mathbf{v}_i), \tag{2}$$

where ε_i is the local site energy, $\mathbf{F}_{ij}$ is the two-body force, and $\mathbf{F}_{ijk}$ is the three-body force. ∇T is the temperature gradient in the length direction, which is defined as $\nabla T = (T_L - T_R)/L$, where T_L, T_R are the temperature of thermostats at the two ends, and L is GNR length. $V = W \cdot d \cdot L$ is the volume, W is the width, and d is the thickness of GNR. In this work we choose $d = 3.35$ Å, which is interplanar spacing of graphite.

We divide the GNR into N slabs in length direction, with each slab containing two GNR layers. The temperature of Jth slab can be calculated from the kinetic energy of atoms according to the Boltzmann distribution:

$$\langle E\rangle = \sum_i^n \frac{1}{2}mv_i^2 = \frac{3}{2}nk_BT_J, \tag{3}$$

where $\langle E\rangle$ is the mean kinetic energy, v_i is the velocity of atom, m is the atomic mass, n is the number of atoms in the slab, and k_B is the Boltzmann constant. We identify the system to get the nonequilibrium stationary state when the averaged temperature and heat flux on each slab do not change with time, and find 5 ns is sufficient in this work. Then we start to calculate the temperature profile and heat flux on GNR by averaging about 5 ns after the nonequilibrium stationary state is set up.

The following four kinds of epitaxial GNRs on SiC are considered: A, SL GNR on SiC (0001); B, BL GNR on SiC(0001); C, SL GNR on SiC ($000\bar{1}$) with the weakly coupled interaction; and D, SL GNR on SiC ($000\bar{1}$) with the covalently bonded interaction. Before geometry optimization, the initial distance between the GNR and SiC surface was set to be 2.3 Å in cases A and B, 3.0 Å in case C, and 2.0 Å in case D.

III. SIMULATION RESULTS AND DISCUSSIONS

In Fig. 1 we show the optimized structures of 8-AGNR on SiC for the above four cases. As one can see, the SL GNRs can either covalently bonded or weakly coupled to the substrate. In the covalently bonded case (cases A, D), the formed C-Si (C-C) covalent bond between GNR and substrate has a length around 2.15 (1.60) Å in the middle region, being consistent with the bond length of the graphene-SiC system in previous reports.[12,13,43] While in the edge region the C-Si (C-C) bond length is only about 2.10 (1.50) Å, shorter than the bond length in the middle region, indicating that the edge atoms make the interaction between GNR and substrate stronger than that between graphene and substrate. In the weakly coupled case (case C), the mean distance between GNR and SiC surface is 3.30 Å, similar with the graphene case.[44]

In the BL GNR (case B), while the mean distance between the first and the second layer is 3.51 Å, it is obviously larger than the interlayer distance of the suspended BL graphene. The larger interlayer distance comes from the larger shear modules

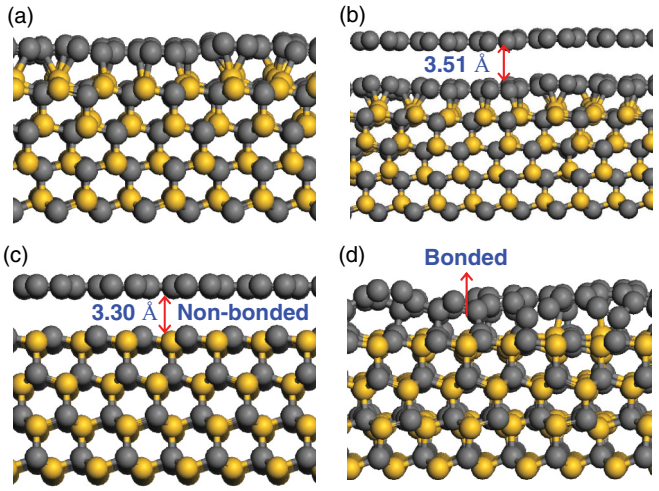

FIG. 1. (Color online) Optimized structures of 8-AGNR on SiC substrate for four cases: (a) single-layer GNR on SiC (0001); (b) bilayer GNR on SiC (0001); (c) single-layer GNR on SiC (000$\bar{1}$) with weakly coupled interaction; and (d) single-layer GNR on SiC (000$\bar{1}$) with covalently bonded interaction. Carbon atoms are represented by gray balls; Si by yellow balls.

of GNRs[45] and the large ripples formed on first GNR layer due to its strong interaction with SiC surface.[46] Compared with the BL graphene, the interlayer force in BL GNR is smaller due to its finite width, while its shear modules are much larger. Thus, unlike the BL graphene, the weak interlayer van der Waals force cannot make the second GNR layer follow the large ripples of the first GNR layer, and the second GNR layer still keeps a relatively planar structure. The large interlayer distance appears at the trough of the ripple in first GNR layer.

The corresponding height profile of GNRs on SiC along the length direction is shown in Fig. 2. From the figure the ripples of GNRs that covalently bonded with SiC are obviously larger than that of GNR weakly coupled with SiC. The smallest and largest ripples appear in cases C and D, respectively, both of which are on SiC (000$\bar{1}$). Moreover, in the BL GNR the ripple of the second GNR layer is obviously smaller than that of first GNR layer [Fig. 2(b)], which corresponds to a larger interlayer distance as discussed above.

Figure 3 shows the width dependence of thermal conductivity of both AGNRs and ZGNRs on SiC. As shown in the figure, the thermal conductivity of GNRs covalently bonded with SiC is very different from that weakly coupled with SiC. In the covalently bonded case, thermal conductivity of GNRs is very low (below 30 W/mK), and has little variation when the width gets larger than 2 nm. This shows that the strong covalent Si-C/C-C bonds formed between GNR and SiC surface have destroyed the intrinsic thermal conductivity of GNRs. In addition, the thermal conductivity of GNR on SiC (000$\bar{1}$) (case D) is distinctly smaller than that on the (0001) surface (case A). This is attributed to the larger GNR ripples formed on the (000$\bar{1}$) surface than that on (0001) surface (Fig. 2), which would induce stronger phonon scattering. Different from the covalently bonded cases, thermal conductivity of GNRs weakly coupled with SiC is much higher (case C). However, we find that some C-Si covalent bonds are newly formed between the edge of SL GNR and SiC (000$\bar{1}$) surface during the NEMD simulation (inset of Fig. 3), which is attributed to the large atomic amplitude of GNR in the direction perpendicular to the SiC surface when the system is thermostated to 300 K. The covalent bonds would induce additional edge localized phonon scattering on the GNR, and thus reduce the thermal conductivity. Since the number of newly formed covalent bonds is proportional to the length of GNR, compared with that of the suspended GNR, we expect the thermal conductivity will be largely reduced when the GNR length gets to micrometer scale (experimental length).

From Fig. 3 it is definite that the thermal conductivity of the second GNR layer in a BL GNR (case B) is very close to that of the suspended GNR. Also, the width dependence of thermal conductivity is very similar to each other: With the width increasing, the thermal conductivity of AGNR monotonously increases, while the thermal conductivity of ZGNR increases first and then decreases.[6] This implies the weak van der Waals

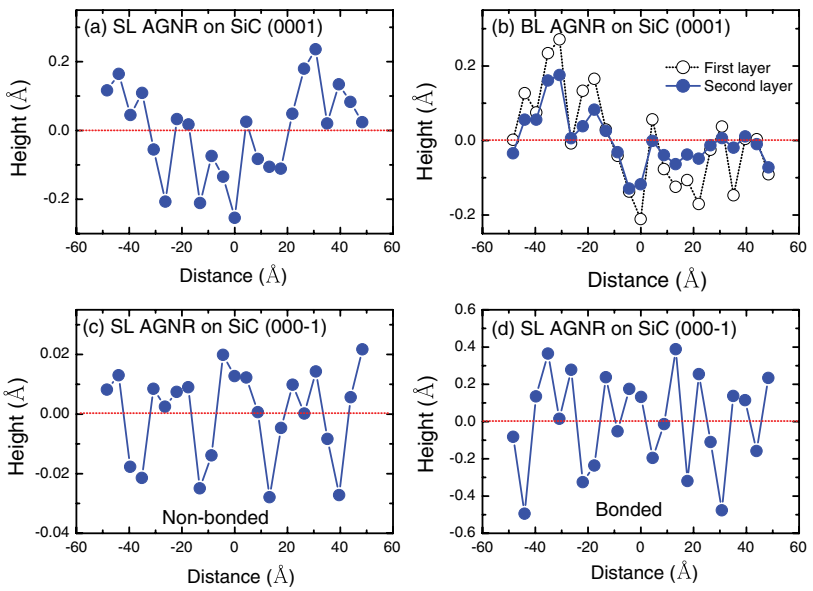

FIG. 2. (Color online) The height profiles of 8-AGNRs on SiC along the length direction for cases (a) A, (b) B, (c) C, and (d) D.

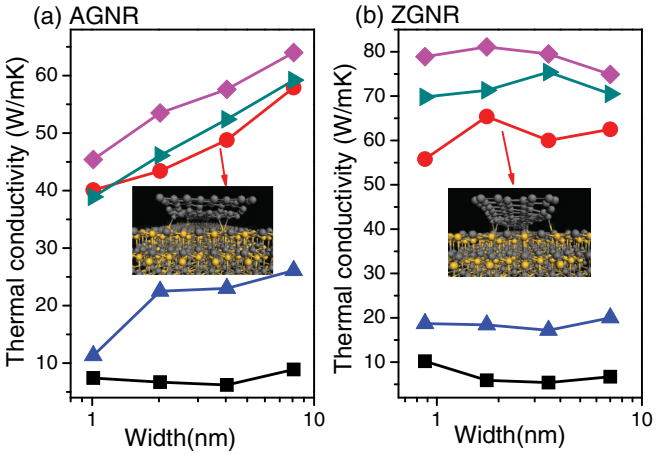

FIG. 3. (Color online) Width dependence of thermal conductivity of both (a) AGNRs and (b) ZGNRs on SiC in cases A (blue up triangle), B (cyan right triangle), C (red circle), and D (black square), with comparison to the suspended GNRs (magenta diamond). The length of GNRs is 10 nm.

interaction from underlying structures (both the first GNR layer and SiC substrate) does not break the intrinsic thermal conductivity of the second GNR layer.

In Fig. 4 we show the length dependence of thermal conductivity of the second layers of BL GNRs with comparison to the suspended GNRs. Similar to that of the suspended GNRs and carbon nanotubes,[6,47] the thermal conductivity of the second 8-AGNR (4-ZGNR) layer monotonously increases with the length increasing and follows a power law of $\kappa \sim L^{\beta}$, with $\beta = 0.38$ (0.49). The value of β is very close to that of the suspended GNR [$\beta = 0.32$ (0.50)], showing that the high thermal conductivity is well preserved in the second GNR layer.

To further explore the substrate effect on thermal conductivity of the second layer of BL GNRs on SiC, we freeze the out-of-plane atomic vibration of the second GNR layer and recalculate the thermal conductivity with comparison to the suspended SL GNR. For simplicity here we only present

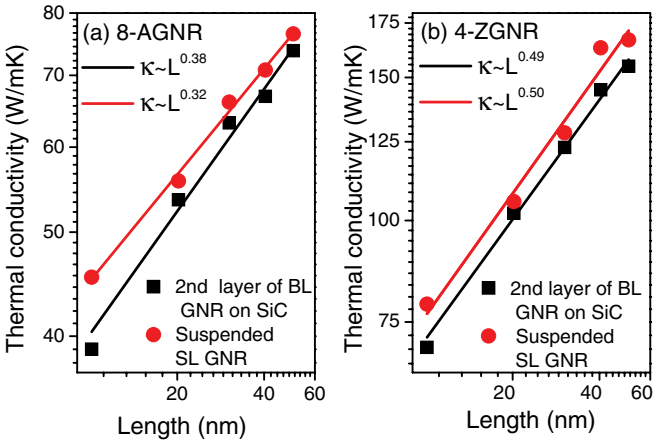

FIG. 4. (Color online) Thermal conductivity κ vs the length L in log-log scale for the second (a) 8-AGNR and (b) 4-ZGNR layers in BL GNR, with comparison to the suspended GNRs. In both cases, $\kappa \sim L^{\beta}$, with β being close to that of the suspended GNRs.

TABLE I. Thermal conductivity κ of 8-ZGNRs with/without the out-of-plane vibrational constraint. The GNR length is kept at 10 nm.

GNR type	Constraint	κ (W/mK)
Suspended SL GNR	Free	81.1
Suspended SL GNR	Constraint	77.7
Second layer of BL GNR	Free	71.3
Second layer of BL GNR	Constraint	79.1

the calculated thermal conductivity of ZGNRs. A similar result is also obtained for AGNRs. As shown in Table I, freezing the out-of-plane atomic vibration decreases the thermal conductivity of the suspended SL GNR, while it considerably increases the thermal conductivity of the second layer of BL GNR.

This illustrates two facts. One is that the out-of-plane phonon mode in suspended SL GNR has a positive contribution to the thermal transport, although it is not dominating. The other is that the thermal conductivity reduction of the second layer of BL GNR mainly comes from the coupling between its out-of-plane phonon mode and the phonon modes of the underlying structures (including phonon modes of both first GNR layer[48] and SiC surface). It should be mentioned that the thermal conductivity of the second layer (79.1 W/mK) in BL GNR is even higher than that of the suspended SL GNR (77.7 W/mK) when the out-of-plane atomic vibration is frozen. This interesting phenomenon indicates an increment of thermal conductivity can be realized through the substrate coupling in system with only two-dimensional vibrations. Recently, through a coupled atomic chain model, we have clarified that there exists a competitive mechanism on thermal conductivity in a coupling system: the phonon resonance effect that decreases thermal conductivity and phonon-band-up-shift effect that increases thermal conductivity.[23] In this case, the phonon resonance effect mainly comes from the coupling between out-of-plane phonon mode of the second GNR layer and the phonon modes of the first GNR layer and SiC substrate. When the out-of-plane atomic vibration is frozen, the phonon resonance effect would be largely reduced, and the phonon-band-up-shift effect become dominated. Thus the thermal conductivity can be increased by the coupling. The results further confirm the existence of two competitive effects between the thermal conductive material and substrate.

To make a more sound connection to experimental systems, where the GNRs are usually with disordered and contaminated

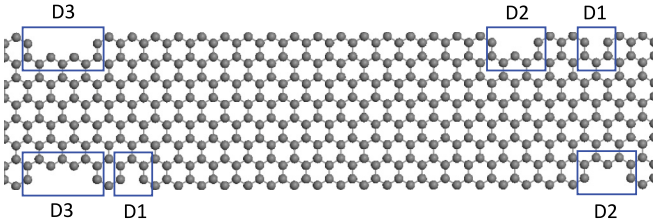

FIG. 5. (Color online) Schematic representation of GNR with disordered edge defects, with single (D1), double (D2), and triple (D3) missing hexagons coexisting on each edge.

TABLE II. Thermal conductivity κ (W/mK) of 8-ZGNRs with/without disordered edge defects on SiC substrate. The GNR length is kept at 10 nm.

GNR type	κ of ideal GNR	κ of defected GNR
Suspended GNR	81.1	30.8
GNR in case A	18.4	14.5
GNR in case B	71.3	29.2
GNR in case C	65.4	26.9
GNR in case D	5.9	5.6

edges, we further calculate thermal conductivity of 8-ZGNR of 10 nm long with three types of defects: single (D1), double (D2), and triple (D3) missing hexagons defects,[49] coexisting on each edge of GNR (remove nine atoms on each edge, see Fig. 5). To give an idea of the impact of disordered defect, we arrange the three types of defects with random position on each GNR edge 12 times, and the final thermal conductivity is averaged over the 12 random cases.

As shown in Table II, the thermal conductivity of all the GNRs decreases with the presence of disordered edge defects. Moreover, the defects have the most dramatically influence on thermal conductivity of suspended GNR, which make the reduction of thermal conductivity get to 62.0% (from 81.1 to 30.8 W/mK). The thermal conductivity reduction in second layer of BL GNR (59.0%) and SL GNR weakly coupled with SiC (58.9%) are also remarkable. However, for the SL GNRs covalently bonded with SiC, the thermal conductivity reduction induced by disordered edge defects is less than 21.0%, not so remarkable. This indicates the disordered edge defects have more significant influence on thermal conductivity of GNRs which have perfect structure and weak interactions with substrate, due to the strong phonon scattering from edge-localized phonons. For the GNRs that have strong interaction with substrate since the intrinsic thermal conductivity of GNRs has been destroyed by the substrate, the effect of disordered edge defects becomes minor.

IV. CONCLUSIONS

In summary, we have investigated the thermal conductivity of epitaxial SL and BL GNRs on SiC substrate using the NEMD method. For the SL GNR, both covalently bonded and weakly coupled GNR-substrate interaction conditions that were observed by experiments are considered. The thermal conductivity of SL GNRs in the covalently bonded conditionis particularly low, while it is much higher in the weakly coupled condition. However, there appear some C-Si covalent bonds between the edge of SL GNR and SiC surface in the weakly coupled condition during the thermal transport, which induces additional edge localized phonon scattering and is expected to largely reduce the thermal conductivity when the GNR length gets to micrometer scale. The second layer of BL GNR is found to have the highest thermal conductivity among all the epitaxial GNRs, and keeps much the same thermal-conductivity characteristics as the suspended GNR. We find that the out-of-plane phonon mode of the second GNR layer plays a critical role on the thermal conductivity variation induced by the underlying structures. The existence of two competitive effects between thermal conductive material and substrate is further confirmed. The effect of disordered edge defects on thermal conductivity of epitaxial GNRs is further investigated. The results show that disordered edge defects can remarkably decrease thermal conductivity of GNRs weakly interacted with substrate, while the effect becomes minor on GNRs strongly interacted with substrate. We expect the present study can be helpful to the forthcoming applications of epitaxial graphene nanomaterials in nanoelectronics.

ACKNOWLEDGMENTS

Z.X.G. acknowledges the support by the Start-up funds (No. 10QDZ11), Scientific Research Fund (10XZX05) of Xiangtan University. J.W.D. wishes to acknowledge support from PCSIRT (IRT1080). X.G.G. acknowledges the support of the Special Funds for Major State Basic Research, National Science Foundation of China, Ministry of Education and Shanghai Municipality.

*zxguo08@gmail.com

[1] A. K. Geim, Science **324**, 1530 (2009).
[2] A. H. Castro Neto, F. Guinea, N. M. R. Peres, K. S. Novoselov, and A. K. Geim, Rev. Mod. Phys. **81**, 109 (2009).
[3] A. A. Balandin, S. Ghosh, W. Bao, I. Calizo, D. Teweldebrhan, F. Miao, and C. N. Lau, Nano Lett. **8**, 902 (2008).
[4] A. A. Balandin, Nat. Mater. **10**, 569 (2011).
[5] J. Hu, X. Ruan, and Y. P. Chen, Nano Lett. **9**, 2730 (2009).
[6] Z. X. Guo, D. Zhang, and X. G. Gong, Appl. Phys. Lett. **95**, 163103 (2009).
[7] K. S. Novoselov, A. K. Geim, S. V. Morozov, D. Jiang, M. I. Katsnelson, I. V. Grigorieva, S. V. Dubonos, and A. A. Firsov, Nature (London) **438**, 197 (2005).
[8] Y. Zhang, Y. W. Tan, H. L. Stormer, and P. Kim, Nature (London) **438**, 201 (2005).
[9] W. A. de Heer, C. Berger, X. S. Wu, P. N. First, E. H. Conrad, X. B. Li, T. B. Li, M. Sprinkle, J. Hass, M. L. Sadowski, M. Potemski, and G. Martinez, Solid State Commun. **143**, 92 (2007).
[10] K. V. Emtsev, F. Speck, T. Seyller, L. Ley, and J. D. Riley, Phys. Rev. B **77**, 155303 (2008).
[11] C. Dimitrakopoulos, Y. M. Lin, A. Grill, D. B. Farmer, M. Freitag, Y. Sun, S. J. Han, Z. Chen, K. A. Jenkins, Y. Zhu, Z. Liu, T. J. McArdle, J. A. Ott, R. Wisnieff, and P. Avouris, J. Vac. Sci. Technol. B **28**, 985 (2010).
[12] A. Mattausch and O. Pankratov, Phys. Rev. Lett. **99**, 076802 (2007).
[13] F. Varchon, R. Feng, J. Hass, X. Li, B. N. Nguyen, C. Naud, P. Mallet, J. Y. Veuillen, C. Berger, E. H. Conrad, and L. Magaud, Phys. Rev. Lett. **99**, 126805 (2007).
[14] S. Kim, J. Ihm, H. J. Choi, and Y. W. Son, Phys. Rev. Lett. **100**, 176802 (2008).
[15] J. H. Seol, I. Jo, A. L. Moore, L. Lindsay, Z. H. Aitken, M. T. Pettes, X. Li, Z. Yao, R. Huang, D. A. Broido, N. Mingo, R. S. Ruoff, and L. Shi, Science **328**, 213 (2010).
[16] W. Jang, Z. Chen, W. Bao, C. N. Lau, and C. Dames, Nano Lett. **10**, 3909 (2010).

[17]Y. K. Koh, M. H. Bae, D. G. Cahill, and E. Pop, Nano Lett. **10**, 4363 (2010).
[18]Z. Wang, R. Xie, C. T. Bui, D. Liu, X. Ni, B. Li, and T. L. J. Thong, Nano Lett. **11**, 113 (2011).
[19]Z. Y. Ong and E. Pop, Phys. Rev. B **84**, 075471 (2011).
[20]F. Hiebel, P. Mallet, F. Varchon, L. Magaud, and J. Y. Veuillen, Phys. Rev. B **78**, 153412 (2008).
[21]Z. X. Guo, D. Zhang, Y. T. Zhai, and X. G. Gong, Nanotechnology **21**, 285706 (2010).
[22]Z. X. Guo and X. G. Gong, Front. Phys. **4**, 389 (2009).
[23]Z. X. Guo, D. Zhang, and X. G. Gong, Phys. Rev. B **84**, 075470 (2011).
[24]Y. W. Son, M. L. Cohen, and S. G. Louie, Phys. Rev. Lett. **97**, 216803 (2006).
[25]J. S. Wang, Phys. Rev. Lett. **99**, 160601 (2007).
[26]Y. Dubi and M. D. Ventra, Rev. Mod. Phys. **83**, 131 (2011).
[27]P. K. Schelling and S. R. Phillpot, and P. Keblinski, Phys. Rev. B **65**, 144306 (2002).
[28]P. G. Klemens and D. F. Pedraza, Carbon **32**, 735 (1994).
[29]Y. J. Han and P. G. Klemens, Phys. Rev. B **48**, 6033 (1993).
[30]D. L. Nika, E. P. Pokatilov, A. S. Askerov, and A. A. Balandin, Phys. Rev. B **79**, 155413 (2009).
[31]A. Ward, D. A. Broido, D. A. Stewart, and G. Deinzer, Phys. Rev. B **80**, 125203 (2009).
[32]L. Lindsay, D. A. Broido, and N. Mingo, Phys. Rev. B **82**, 115427 (2010).
[33]N. Wei, L. Xu, H. Q. Wang, and J. C. Zheng, Nanotechnology **22**, 105705 (2011).
[34]S. Chien, Y. T. Yang, and C. K. Chen, Appl. Phys. Lett. **98**, 033107 (2011).
[35]C. Riedl and U. Starke, J. Bernhardt, M. Franke, and K. Heinz, Phys. Rev. B **76**, 245406 (2007).
[36]J. Tersoff, Phys. Rev. B **39**, 5566 (1989).
[37]J. I. Iwata, D. Takahashi, A. Oshiyama, B. Boku, K. Shiraishi, S. Okada, and K. Yabana, J. Comput. Phys. **229**, 2339 (2010).
[38]L. Wirtz and A. Rubio, Solid State Commun. **131**, 141 (2004).
[39]L. A. Girifalco, M. Hodak, and R. S. Lee, Phys. Rev. B **62**, 13104 (2000).
[40]Z. Mao, A. Garg, and S. B. Sinnott, Nanotechnology **10**, 273 (1999).
[41]S. Nosé, J. Chem. Phys. **81**, 511 (1984); W. G. Hoover, Phys. Rev. A **31**, 1695 (1985).
[42]N. Yang, G. Zhang, and B. Li, Nano Lett. **8**, 276 (2008).
[43]Y. Qi, S. H. Rhim, G. F. Sun, M. Weinert, and L. Li, Phys. Rev. Lett. **105**, 085502 (2010).
[44]F. Hiebel, P. Mallet, J. Y. Veuillen, and L. Magaud, Phys. Rev. B **83**, 075438 (2011).
[45]R. Faccio, P. A. Denis, H. Pardo, C. Goyenola, and Á. W. Mombrú, J. Phys.: Condens. Matter **21**, 285304 (2009).
[46]F. Varchon, P. Mallet, J. Y. Veuillen, and L. Magaud, Phys. Rev. B **77**, 235412 (2008).
[47]S. Maruyama, Physica B **323**, 193 (2002).
[48]H. Y. Cao, Z. X. Guo, H. J. Xiang, and X. G. Gong, Phys. Lett. A **376**, 525 (2012).
[49]A. Cresti and S. Roche, Phys. Rev. B **79**, 233404 (2009).